



HAL
open science

Polymerization of epoxide monomers promoted by t BuP 4 phosphazene base: a comparative study of kinetic behavior

Valentin Puchelle, Haiqin Du, Nicolas Illy, Philippe Guégan

► **To cite this version:**

Valentin Puchelle, Haiqin Du, Nicolas Illy, Philippe Guégan. Polymerization of epoxide monomers promoted by t BuP 4 phosphazene base: a comparative study of kinetic behavior. *Polymer Chemistry*, 2020, 11 (21), pp.3585-3592. 10.1039/D0PY00437E . hal-03158435

HAL Id: hal-03158435

<https://hal.science/hal-03158435>

Submitted on 10 Mar 2021

HAL is a multi-disciplinary open access archive for the deposit and dissemination of scientific research documents, whether they are published or not. The documents may come from teaching and research institutions in France or abroad, or from public or private research centers.

L'archive ouverte pluridisciplinaire **HAL**, est destinée au dépôt et à la diffusion de documents scientifiques de niveau recherche, publiés ou non, émanant des établissements d'enseignement et de recherche français ou étrangers, des laboratoires publics ou privés.

Polymerization of epoxide monomers promoted by $t\text{BuP}_4$ phosphazene base: A comparative study of kinetic behavior.

Valentin Puchelle,^a Haiqin Du,^a Nicolas Illy^{*a} and Philippe Guégan^{*a}

Received 00th January 20xx,
Accepted 00th January 20xx

DOI: 10.1039/x0xx00000x

Kinetics of the anionic ring-opening polymerizations (AROP) of epoxide monomers, 1,2-epoxybutane (BO), 1,2-epoxypropane (PO), *tert*-butyl glycidyl ether (*t*BuGE), allyl glycidyl ether (AGE), benzyl glycidyl ether (BnGE), ethoxyethyl glycidyl ether (EEGE) were investigated using benzyl alcohol / $t\text{BuP}_4$ as initiating system. All the polymerizations proceed in a controlled manner following a first order kinetic with respect to the monomer. Influence of the side chains born by the oxirane ring was evidenced. Propagating centers derived from epoxide bearing heretoatom-containing side chains display higher reactivities and propagation rates. A reactivity scale has been established and is as follow, $k_{p,\text{BnGE}} > k_{p,\text{AGE}} > k_{p,\text{EEGE}} \gg k_{p,\text{tBuGE}} \approx k_{p,\text{PO}} > k_{p,\text{BO}}$. Using BO as model monomer and different initiator concentrations, the nature of the propagating species has been identified as ion pairs. The influence of a Lewis acid addition on the monomer reactivities and on the control of the polymerization was also investigated. In the presence of triisobutylaluminum (*i*Bu₃Al), polymerization kinetics were faster but led to a broadening of the molar masses distributions. The monomer reactivity scale was also strongly modified with $k_{p,\text{PO}} > k_{p,\text{BO}} > k_{p,\text{EEGE}} \approx k_{p,\text{AGE}} > k_{p,\text{BnGE}} \approx k_{p,\text{tBuGE}}$. The polymerizations of PO, BO and *t*BuGE follow zero order kinetics which is not the case of the other oxirane monomers.

Introduction

Polyethers exhibit specific characteristics, such as low glass transition temperatures and hydrophilicity. Thus, they find applications in a wide range of fields ranging from biomedical science to solar energy harvesting or energy storage in battery.¹⁻³ Polyethers are commonly synthesized by AROP of epoxide monomers initiated by either alkali metal derivatives such as hydrides or alkoxides combined with metal counter ions.⁴⁻⁶ However, since the beginning of 2010's, organocatalyzed polymerization has gain interest and recent developments have been applied to AROP.⁷⁻¹⁰ Organocatalysts allow in particular to enhance the propagation rates and to improve the selectivity of the polymerization toward competing reactions. Among the large variety of commercially-available organocatalysts, the extremely strong, sterically hindered, nonionic phosphazene bases are of particular interest due to their ability to strongly increase the polymerization rates and to access new macromolecular architectures.¹¹ Tetrameric phosphazene base $t\text{BuP}_4$ is able to deprotonate very low acidic molecules (XH), generating extremely reactive anions associated with very large, highly

stable, soft phosphazanium cations. The range of chemical moieties used as initiators in combination with $t\text{BuP}_4$ has been extended to carboxylic acids,¹² thiols,¹³ CH acidic compounds,¹⁴ or nitrogen containing functions such as primary,¹⁵ secondary amides¹⁶⁻¹⁸ or carbamates.¹⁹ In particular, Möller and coworkers were the first to demonstrate the ability of these superbases to initiate the AROP of ethylene oxide using alcohol initiator.²⁰ Alcohol moiety is probably one of the most commonly found chemical functional group. Thus, $t\text{BuP}_4$ - alcohol initiating systems have then been extended to several oxirane monomers, such as 1,2-epoxypropane (PO), 1,2-epoxybutane (BO), ethoxyethyl glycidyl ether (EEGE), benzyl glycidyl ether (BnGE), *tert*-butyl glycidyl ether (*t*BuGE) and glycidylamine derivatives.^{2, 21-23} To the best of our knowledge, $t\text{BuP}_4$ is the only organic base that has been successfully used with alcohols as initiating systems for the polymerization of epoxides. Polymerization did not occurred with milder organic bases such as $t\text{BuP}_1$, $t\text{BuP}_2$, TBD, DBU, TIBP or MTBD.^{2, 14, 20, 21, 24, 25} In order to increase the reactivity of the system and lower the transfer reaction occurrence, Carlotti and coworkers were the first to combine alcohol- $t\text{BuP}_4$ initiating systems with a Lewis acid, tri-isobutylaluminum (*i*Bu₃Al), to initiate the AROP of propylene oxide, and perform an activated monomer mechanism with oxirane monomer family.²⁶ Unfortunately, even if numerous papers described the polymerization of epoxides initiated by alcohol- $t\text{BuP}_4$ or by alcohol- $t\text{BuP}_4$ -*i*Bu₃Al initiating systems, few kinetics data, such as propagation rate constants, are available. A comparison of the different epoxide monomer reactivities in the presence of $t\text{BuP}_4\text{H}^+$ phosphazanium counter-ions is very difficult due to the variety

^a Sorbonne Université, CNRS, Institut Parisien de Chimie Moléculaire, Equipe Chimie des Polymères, 4 place Jussieu, F-75005 Paris, France.

E-mail: nicolas.illy@sorbonne-universite.fr, philippe.guegan@sorbonne-universite.fr

† Footnotes relating to the title and/or authors should appear here.

Electronic Supplementary Information (ESI) available: [details of any supplementary information available should be included here]. See DOI: 10.1039/x0xx00000x

of experimental conditions used in the literature. A rational study involving most common monomers under standardized reaction conditions is lacking. In addition, to the best of our knowledge, the nature of the propagating species involved in the presence of phosphazanium as counter ion has not been elucidated.

In this work, we aim to address these gaps in fundamental knowledge, and to provide a rational study involving the most common epoxide monomers. The AROP of 6 different epoxides, namely PO, BO, AGE, EEGE, BnGE and *t*BuGE, were carried out under identical reaction conditions with benzyl alcohol-*t*BuP₄ as initiating system. Kinetic studies have been performed, and the propagation rate constants have been calculated. The reactivities of epoxides have been compared and the influence of the chemical nature, the electron density and the steric hindrance of the lateral substituents have been highlighted. The nature of the phosphazanium alkoxide propagating species has been investigated using BO as model monomer. In the last part, kinetic studies were performed under the same conditions but in the presence of *i*Bu₃Al Lewis acid, under activated monomer mechanism conditions. A monomer reactivity scale has been established and compared with the previous one.

Experimental

Materials and methods. Benzyl alcohol (anhydrous, 99.8%, Sigma-Aldrich), phosphazene base *t*BuP₄ solution (0.8 mol.L⁻¹ in hexane, Sigma-Aldrich), triisobutyl aluminum (*i*Bu₃Al) solution (1 mol.L⁻¹ in hexane), 2-methyltetrahydrofuran (MeTHF) (98%, Sigma-Aldrich) were used as received. 1,2-epoxybutane (>99%, Sigma-Aldrich), 1,2-epoxypropane, (≥99.5, Sigma-Aldrich), *tert*-butyl glycidyl ether (99%, Sigma-Aldrich), allyl glycidyl ether (≥99%, Sigma-Aldrich) were distilled over CaH₂ (93%, 0-2 mm grain size, Acros Organic) two times prior to use. Benzyl glycidyl ether (99%, Sigma-Aldrich) was dried over activated molecular sieves (3 Å). Tetrahydrofuran was dried with an MBRAUN MB SPS-800 solvent purification system under nitrogen. Ethoxyethyl glycidyl ether was synthesized from glycidol and ethyl vinyl ether following the procedure reported by Fitton and al.²⁷ and distilled twice over CaH₂ prior to use.

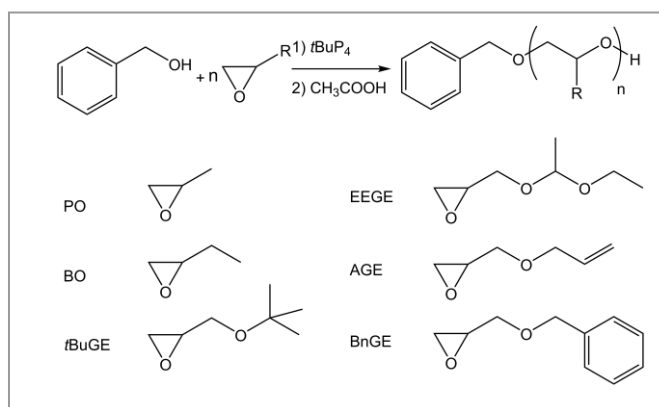
Instrumentation. ¹H analyses were performed on a Bruker Avance 300 MHz spectrometer. CDCl₃ was used as deuterated solvent. Polymer molar masses were determined by Size Exclusion Chromatography (SEC) with three PLGel Mixte C 5 μm columns (7.5 x 300 mm; separation limits: 0.2-2000 kg.mol⁻¹) maintained at 40°C coupled with two modular detectors: a differential refractive index (RI) detector Viscotek 3580 and a Diode Array UV detector Shimadzu SPD20-AV. THF was used as the mobile phase at a flow rate of 1 ml.min⁻¹, toluene was used as a flow rate marker. All polymers were injected (100 μl) at a

concentration of 5 mg.ml⁻¹ after filtration through a 0.45 μm pore-size membrane. OmniSEC 4.7 software was used for data acquisition and data analysis. The number-average molar masses (*M*_n), the weight-average molar masses (*M*_w) and the molar mass distribution ($\mathcal{D} = M_w/M_n$) were determined by SEC with a calibration curve based on narrow poly(methyl methacrylate) (PMMA) standards (from Polymer Standard Services), using the RI detector.

Matrix-Assisted Laser Desorption and Ionization Time-of-Flight Mass spectra were recorded by matrix-assisted laser desorption and ionization time-of-flight (MALDI-ToF) mass spectrometry (MS) using a Bruker autoflex III smartbeam mass spectrometer, equipped with the laser that produces pulses at 337 nm using dithranol as a matrix and NaI as cationizing agent. Spectra were recorded in reflectron and linear mode at an accelerating potential of 20 kV. Samples were prepared by dissolving the polymer in THF at a concentration of 5 mg.ml⁻¹. A 10 μL aliquot of this solution was mixed with 20 μl of dithranol solution as matrix (at 20 mg.ml⁻¹ in THF) and 10 μl of NaI solution (at 10 mg.ml⁻¹ in THF). Standards (poly(ethylene oxide) of known structures, *M*_n = 1470 g.mol⁻¹ purchased from Polymer Standards Service) were used to calibrate the mass scale.

Procedures. All polymerization were carried out at 25°C, under nitrogen in a glass reactor fitted with a Rotaflo and equipped with a stirring bar and closed with a septum. The following typical procedure was applied. In a glove box, the phosphazene base *t*BuP₄ solution (242 μl, 0.194 mmol) was introduced into the polymerization reactor. Then hexane was evaporated using high vacuum from a vacuum line (≈ 10⁻⁶ hPa). Reaction vessel was transferred back into the glovebox and dried THF was added (4.15 ml) followed by benzyl alcohol (20 μl, 0.193 mmol). Finally, the monomer BO was added (840 μl, 9.66 mmol). After closure of the reactor, the reaction was stirred at 25°C and left to react for the required period of time. For polymerization carried out in the presence of *i*Bu₃Al, the Lewis acid was added after *t*BuP₄ and just before the monomer. It may be noted that the addition of *i*Bu₃Al provoked a temporary rise of the temperature inside the reaction vessel above 25°C. Kinetic studies were followed by removing aliquots at various reaction times, conversion and molar masses were determined by ¹H NMR and by SEC, respectively (Figures S1-S11). The reaction was quenched by addition of 0.1 ml of acid acetic 10%. The polymer was dissolved in chloroform and purified by passing through aluminum oxide and by removing the solvent under vacuum at 50°C to give a colorless viscous liquid. Yield ≥ 80%. Kinetic experiments were run at least twice to confirm the behavior of each monomer towards the initiating system considered.

Results and discussion



Scheme 1 $t\text{BuP}_4$ catalyzed AROP of oxirane monomers using $\text{BnOH}:\text{tBuP}_4$ as initiating system.

Ring-opening polymerizations of alkyl-substituted epoxides (PO, BO) and glycidyl ether monomers ($t\text{BuGE}$, EEGE , AGE , BnGE) were first performed under N_2 atmosphere with benzyl alcohol: $t\text{BuP}_4$ as initiating system (Scheme 1). These epoxide monomers are among the most common epoxide monomers used to prepare well-defined polyethers.² The monomer concentration was fixed to $[\text{M}]_0 = 2 \text{ mol.L}^{-1}$ and the $[\text{tBuP}_4]_0/[\text{initiator}]_0$ ratio was fixed to 1/1. A reaction temperature of 25°C was chosen and is expected to ensure reaction completion in a reasonable amount of time. Preliminary experiments dealing with the nature of the propagating species were conducted with BO, a quite safe monomer providing the usual characteristics of substituted epoxide.

Investigation of the nature of the propagating species

First, the chemical nature identification of the propagating centers was carried out. Various $[\text{BO}]_0/[\text{Initiator}]_0$ ratios were used, and the $[\text{tBuP}_4]_0/[\text{initiator}]_0$ ratio set to 1 (Table 1). Initiator concentration $[\text{I}]_0$ ranged from 7.5 mmol.L^{-1} to 60 mmol.L^{-1} for a fixed monomer concentration $[\text{M}]_0 = 2.0 \text{ mol.L}^{-1}$. Kinetic data could be fitted according to a first-order equation. For all $[\text{M}]_0/[\text{I}]_0$ ratios, the reactions were first order with respect to the monomer over the entire conversion range

(Figure 1), which is in good agreement with previously reported results for AROP of BO initiated by low acidic molecules- $t\text{BuP}_4$ initiating systems.^{16, 22}

Furthermore, the poly(BO) molar mass increases linearly with the monomer conversion up to final yield. Experimental molar masses M_n are in good agreement with the theoretical values and dispersity \mathcal{D} remains narrow over the entire conversion range. These results are illustrated in Figure S13, which corresponds to experimental data obtained for $[\text{M}]_0/[\text{I}]_0$ ratio = 50/1 (Table 1 run 4), but the conclusion applies equally well to the five $[\text{M}]_0/[\text{I}]_0$ ratios. The above kinetic results argue in favor of a living polymerization mechanism occurring without transfer or termination reactions under the investigated conditions. Kinetic results obtained for all the $[\text{M}]_0/[\text{I}]_0$ ratios are superimposed on a pseudo first order plot (Figure 1). A linear dependence regarding $\ln([\text{M}]_0/[\text{M}])$ versus time can be observed for each ratio. From each curve, a value of propagating constant $k_{p, \text{app}}$ was determined using the slope ($k_p[\text{I}]_0$) of the linear regression.

Anionic polymerization in polar organic solvent proceeds via a

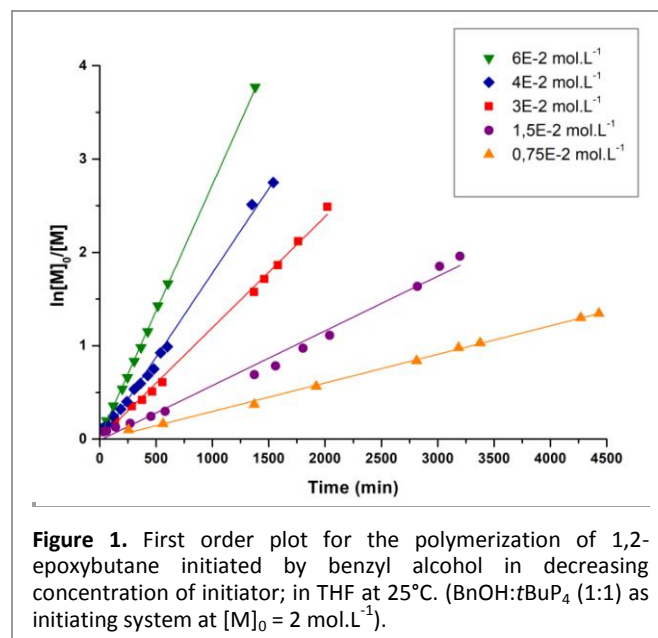


Figure 1. First order plot for the polymerization of 1,2-epoxybutane initiated by benzyl alcohol in decreasing concentration of initiator; in THF at 25°C . ($\text{BnOH}:\text{tBuP}_4$ (1:1) as initiating system at $[\text{M}]_0 = 2 \text{ mol.L}^{-1}$).

Table 1. 1,2-epoxybutane polymerization, initiated by benzyl alcohol: $t\text{BuP}_4$ (1:1) at 25°C in THF; $[\text{M}]_0 = 2.0 \text{ mol.L}^{-1}$.^a Determined by ^1H NMR in CDCl_3 ; ^b Slope of the curves in Figure 3.

Run	$[\text{BnOH}]_0$ ($10^{-2} \text{ mol.L}^{-1}$)	$[\text{BO}]/[\text{BnOH}]/[\text{tBuP}_4]$	Time	% _{Conv} ^a	$k_p[\text{I}]_0$ ^b (min^{-1})	k_p ($10^{-2} \text{ L.mol}^{-1}.\text{min}^{-1}$)
1	0.75	267/1/1	73h50	74	3.06×10^{-4}	4.08
2	1.5	133/1/1	53h15	86	5.85×10^{-4}	3.90
3	3	67/1/1	33h40	92	1.19×10^{-3}	3.96
4	4	50/1/1	22h30	94	1.80×10^{-3}	4.51
5	6	33/1/1	23h	98	2.70×10^{-3}	4.50

multiple state mechanism involving contact ions, solvent separated ion pairs and free anions.²⁸ Szwarc and Schulz have demonstrated that the overall polymerization rate constant, k_p , is function of the concentration of active species (c^*) according to the equation (1) where k_{\pm} is the rate constant of the ion pairs (contact and solvent separated ion pairs), k is the rate constant of free ions and K_D is the overall dissociation constant between the total concentration of ion pairs and free ions.²⁸⁻³⁰

$$k_p = k_{\pm} + (k_- - k_{\pm})K_D^{1/2} (c^*)^{-1/2} \quad (1)$$

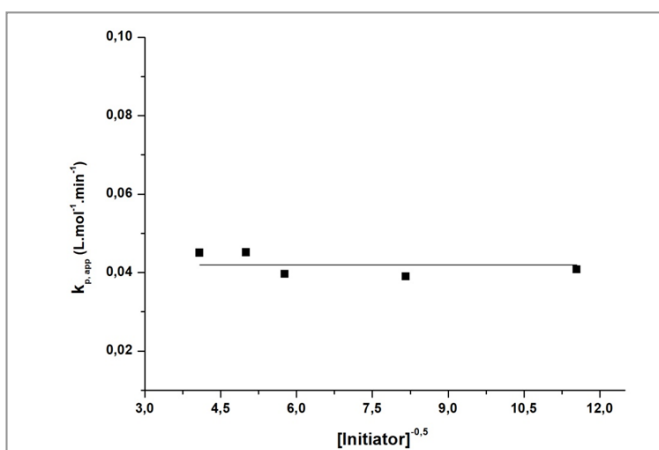


Figure 2. Dependence of the propagation rate constant $k_{p,app}$ towards the reciprocal square root concentration of benzyl alcohol for BO polymerization in THF at 25°C.

In order to determine the contribution of the different propagating species, we plotted $k_{p,app} = f([I]^{0.5})$. Figure 2 shows that $k_{p,app}$ is constant with respect to the reciprocal square root concentration of benzyl alcohol initiator and has an average value of 0.0419 ± 0.0026 L.mol⁻¹.min⁻¹. This result suggests that the propagating active species are exclusively ion pairs. For the polymerization of BO in non-polar toluene, the $k_{p,app}$ values reported by Dentzer et al.¹⁶ and by Misaka et al.²¹ using secondary amide-*t*BuP₄ and alcohol-*t*BuP₄ as initiating systems are equal to 0.0336 L.mol⁻¹.min⁻¹ and 0.0480 L.mol⁻¹.min⁻¹, respectively. Propagation rate constants have very similar values in THF and in toluene, suggesting comparable interactions between H*t*BuP₄⁺ counter-ions and alkoxides in both solvents and that ion pairs are mainly contact ion pairs.

Influence of the epoxide substituent on the propagation rates

Kinetic experiments were carried out with 6 epoxide monomers in THF at 25°C using benzyl alcohol:*t*BuP₄ as initiating system (Table 2 and Figures S12-S17). Poly(propylene oxide) (polyPO, Table 2 run 1), poly(butylene oxide) (polyBO, Table 2 run 2), poly(*tert*-butyl glycidyl ether) (poly*t*BuGE, Table 2 run 3), poly(allyl glycidyl ether) (polyAGE, Table 2 run 4), poly(ethoxyethyl glycidyl ether) (polyEEGE, Table 2 run 5) and poly(benzyl glycidyl ether) (polyBnGE, Table 2, run 6) were successfully synthesized with very narrow dispersities. For all runs, experimental number-average molar masses measured by end-group analysis of the ¹H NMR spectra are in excellent agreement with the theoretical ones. We can thus conclude that the initiation is quantitative and that each benzyl alcohol molecule generates one macromolecule. In addition, the M_n of polyPO, polyBO, polyAGE, and polyEEGE determined by SEC in THF are also in very good agreement with the theoretical number-average molar masses, suggesting the absence or a negligible amount of transfer reactions. A discrepancy can be noticed in the case of polyether bearing bulky hydrophobic lateral substituents like poly*t*BuGE and of polyBnGE. However, the dispersity remains low for each sample. A first explanation could be that SEC in THF using PMMA standards significantly underestimated the molar masses for these polyethers. In all cases, the reactions were first order with respect to the monomer over the entire conversion range, and the degrees of polymerization increased linearly with conversion over the same conversion range as shown in Figures S12-S17. The above kinetic results, coupled to the very narrow molar mass distributions ($\mathcal{D} < 1.1$), provide experimental evidences that support a living and controlled polymerization mechanism (no transfer or termination reactions) and a fast initiation step under the investigated experimental conditions and bearing in mind the relatively low targeted molar masses.

The first order kinetic graphs of the AROP of the six epoxide monomers are superimposed in Figure 3, 2 distinctive groups having propagation rate constants with similar orders of magnitude are clearly visible: (i) BnGE, AGE and EEGE are the most reactive monomers having propagation rate constants ranging from 2.23 to 4.12×10^{-1} L.mol⁻¹.min⁻¹; (ii) BO, PO and *t*BuGE are less reactive having propagation rate constants ranging from 4.51 to 5.43×10^{-2} L.mol⁻¹.min⁻¹. The monomer reactivity order determined here with BnOH-*t*BuP₄ initiating system is: $k_{p,BnGE} > k_{p,AGE} > k_{p,EEGE} \gg k_{p,tBuGE} \approx$

Table 2. Ring-opening polymerization of epoxide monomers initiated by Benzyl Alcohol:*t*BuP₄ (1:1) at 25°C in THF; $[M]_0 = 2$ mol.L⁻¹.

Run	Monomer	Time	% _{Conv}	$k_{p,app}$ (L.mol ⁻¹ .min ⁻¹)	$M_{n,theo}$ (g.mol ⁻¹)	$M_{n,NMR}$ (g.mol ⁻¹)	$M_{n,SEC}$ (g.mol ⁻¹)	M_w/M_n (SEC)
1	PO	25h	96	5.38×10^{-2}	2800	2800	2900	1.09
2	BO	22h30	92	4.51×10^{-2}	3400	3200	3100	1.09
3	<i>t</i> BuGE	22h40	94	5.43×10^{-2}	6200	6100	4900	1.10
4	AGE	4h	96	3.00×10^{-1}	5600	5700	5100	1.08
5	EEGE	5h	94	2.23×10^{-1}	7000	7400	6200	1.08
6	BnGE	4h30	99	4.12×10^{-1}	8200	N.A	4700	1.08

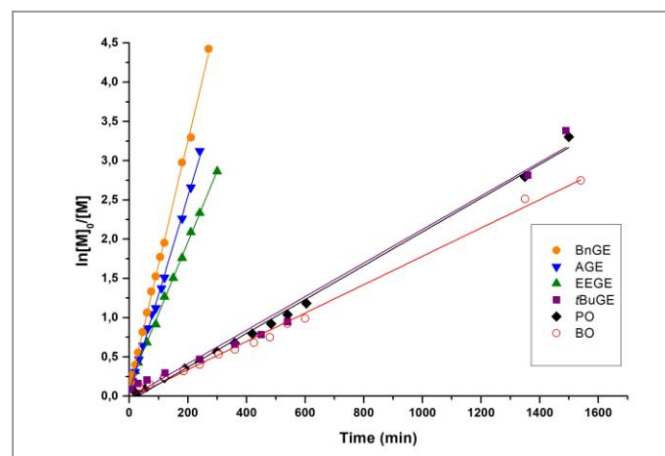


Figure 3. First-order-plot in the polymerization of BnGE, AGE, EEGE, *t*BuGE, PO, BO at 25°C in THF. Monomer/Initiator = 50/1, [Monomer] = 2.0 mol.L⁻¹.

$k_{p,PO} > k_{p,BO}$. When a potassium hydride suspension in THF with 18-crown-6 is used as initiating system, a similar tendency was observed by Stolarzewicz et al.³¹ with $k_{p,AGE} \gg k_{p,PO} > k_{p,BO}$. But, it is worth noting that the monomer reactivity scale is also strongly dependent of the initiating system as illustrated by the results obtained by Möller et al.³² in diglyme at 120°C using potassium 3-phenyl-1-propanol as initiator where $k_{p,EEGE} > k_{p,AGE} > k_{p,tBuGE}$.

We previously demonstrated that only one propagating specie exists in the case of the polymerization of BO, and we suggest a similar trend for *t*BuGE, PO. However, polymerizations of BnGE, AGE, EEGE provide much faster kinetics, that seem to follow a similar behavior. The reactivity differences between the two sets of monomers could be explained by the interactions between the alkoxide propagating center and the counter-ion phosphazanium $HtBuP_4^+$. It is known that the anionic ring-opening polymerization mechanism is based on a tri-molecular transition state valid for ionic pairs propagating species.³³ This state of transition is composed of the propagating center, the counter cation and a monomer unit. The phosphazene base is acting like a Lewis acid and interacts with the following nucleophilic species: the oxanionic

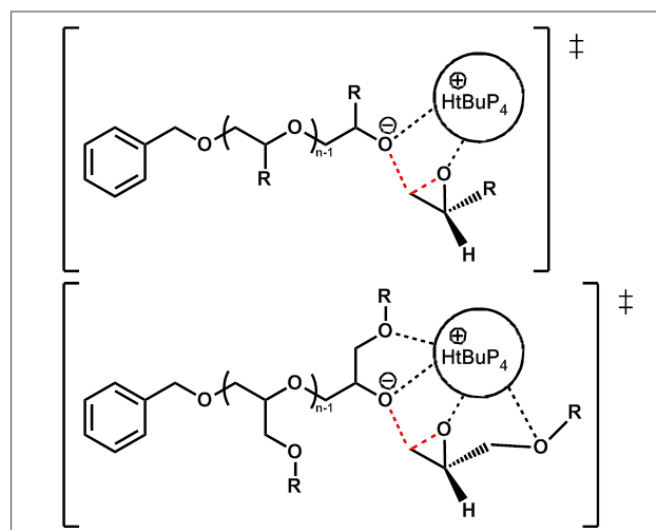


Figure 4. Transition-state structure scheme for the monomer addition regarding the substituent on the epoxide.

propagating center and the monomer unit to be incorporated in the chain as shown in Figure 4. The coordination between alkoxide and $HtBuP_4^+$ stabilizes the transition state and initiates the epoxide cleavage.³⁴ The substituents present on the monomer are known to play an important role in the transition state³⁵ which is confirmed in our case. The methyl and ethyl groups of PO and BO do not interact with the phosphazanium counter-ion in the transition state (Figure 4). On the contrary, in the case of BnGE, EEGE and AGE, multiple interactions are possible between the counter-ion $HtBuP_4^+$ and the oxygen atoms in β -position of the lateral group of the last propagating chain monomer unit and of the monomer being incorporated (Figure 4). These additional interactions tend to weakened the main alkoxide – $HtBuP_4^+$ interaction and thus to increase the nucleophilicity of the alkoxide propagating center and thus, the propagation rate. A similar effect has already been observed for the sodium phenolate initiated AROP of methyl glycidyl ether and thiomethyl glycidyl ether compared to the one of propylene oxide.³⁵ More recently Lynd and coll. published a DFT calculation study reporting that for the AROP

Table 3. Monomer-activated ring-opening polymerization of epoxides initiated by benzyl alcohol: $tBuP_4$: Bu_3Al (1:1:2) at 25°C in THF; $[M]_0 = 2 \text{ mol.L}^{-1}$.

Run	Monomer	Time (min)	%Conv	$M_{n,theo}$ ($g.mol^{-1}$)	$M_{n,NMR}$ ($g.mol^{-1}$)	$M_{n,SEC}$ ($g.mol^{-1}$)	M_w/M_n (SEC)
1	BO	5	92	3400	3700	4800	1.52
2	PO	2,5	96	2900	3300	5400	1.54
3	<i>t</i> BuGE	22	81	5400	8000	7900	1.38
4	AGE	6	85	4900	7700	9900	1.43
5	EEGE	9	94	7000	7200	6700	1.59
6	BnGE	24	85	7100	N.A	5700	1.35

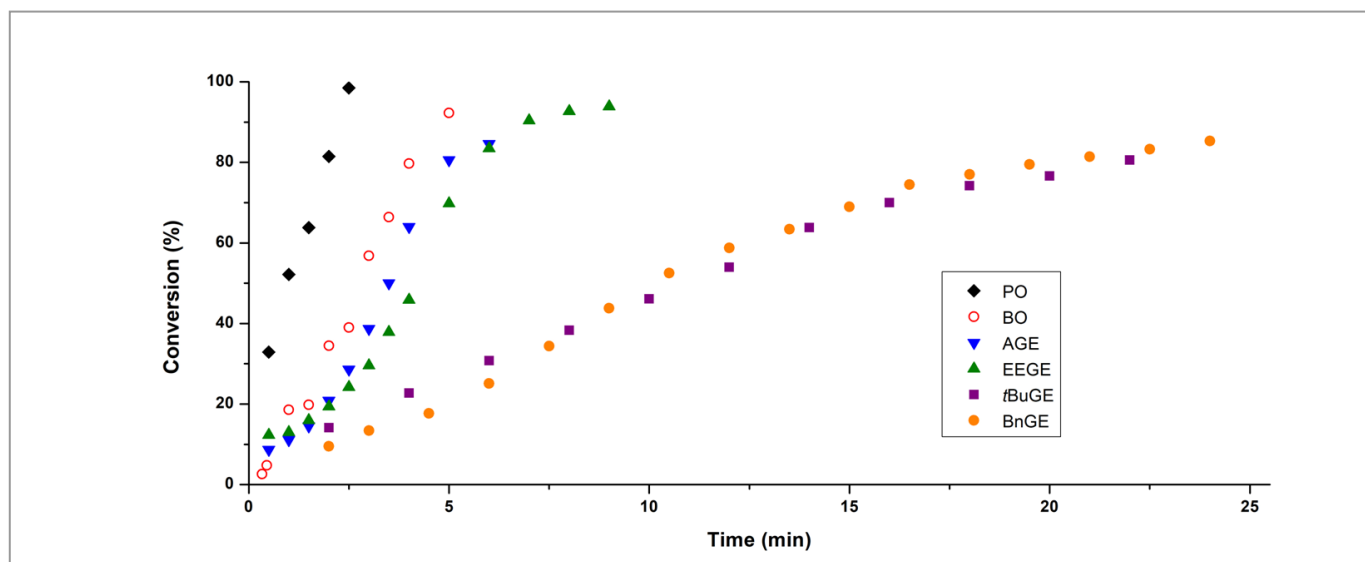


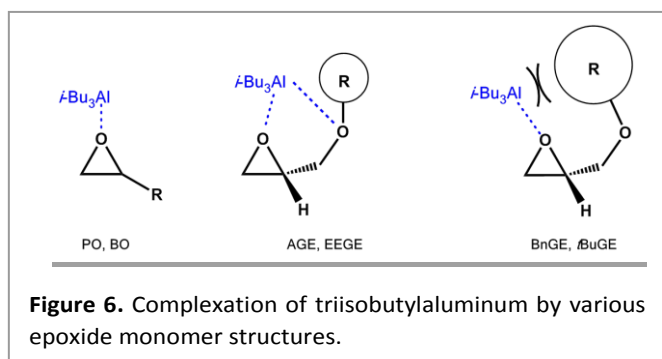
Figure 5. Conversion versus time plots for the polymerization of alkylene oxide monomers BO and PO and for the protected glycidol monomers AGE, EEGE, *t*BuGE, BnGE. (MeTHF, 25°C, $[M]_0 = 2 \text{ mol.L}^{-1}$, $[\text{benzyl alcohol}] = 3,7 \times 10^{-2} \text{ mol.L}^{-1}$, Benzyl alcohol:*t*BuP₄:*i*Bu₃Al (1:1:2)).

initiated by potassium alkoxide, the energetic transition state barrier was lower in the case of the addition of one AGE unit than one EO unit.³⁶ It can be noted that *t*BuGE has a propagation rate constant similar to those of PO and BO despite the presence of an oxygen atom in β position of its lateral substituent. We assume that in this case, the steric hindrance due to the bulky *tert*-butyl group prevents the coordination effect with the bulky phosphazanium counterion.

Polymerization in the presence of a Lewis acid

In this part, the influence of the addition of a Lewis acid in the reaction mixture will be investigated. To the best of our knowledge, no kinetic studies have ever been reported for the AROP of epoxide using a phosphazene base/*i*Bu₃Al as polymerization promoter. Polymerizations were carried out at the same monomer concentration in MeTHF at 25°C with alcohol:*t*BuP₄:*i*Bu₃Al (1:1:2) as catalytic system (Table 3). The solvent was switched from THF to 2-methyltetrahydrofuran (MeTHF), to avoid competitive complexation of the aluminum compound by THF.³⁷ As previously reported,³⁸ a ratio of $[\textit{iBu}_3\text{Al}]/[\text{benzyl alcohol}] > 1$ is required: one equivalent of aluminum derivative is consumed by the low-reactive propagating center, the excess activates the monomer and allows for the propagation. As expected compared to the polymerization without *i*Bu₃Al, the addition of a Lewis acid leads to faster kinetics. However for these moderate targeted polymerization degrees, a loss of polymerization control suggested by the increase of the dispersity ($1.35 < \bar{M}_w < 1.60$) are concomitantly observed (Figure S18). All the samples were analyzed by MALDI TOF: only the expected populations could be detected (Supporting Information Figures S25-S30) suggesting living polymerization mechanisms without transfer reactions.

In order to determine the monomer order, monomer conversion and $\ln([M]_0/[M])$ were plotted as function of time (Figures S19-S24). All the polymerizations proceed at high speed: less than 30 minutes were actually needed to reach full conversion. The polymerization of PO, BO and *t*BuGE were zero-order with respect to the monomer. These results are similar to the ones obtained by Carloti and coll. who have reported that the polymerizations of PO with alkoxide/*i*Bu₃Al,³⁸ onium salt/*i*Bu₃Al,³⁹ and tetraalkylammonium salt/*i*Bu₃Al as initiating systems⁴⁰ are following a zero order kinetics according to the equation $R_p = k_p [I]_0 \cdot ([i\text{Bu}_3\text{Al}]_0 - [I]_0)$ where k_p is the propagation rate constant and $[I]_0$ the initiator concentration. For AGE, EEGE and BnGE, kinetic data could not be fitted according to a zero order equation or a first order equation. Carloti suggests that *an induction period is observed at the early stage, and could be explain by the aggregation of complexes between low molar mass propagating macromolecules, phosphazanium counter-ion and iBu₃Al*. After the insertion of few additional monomer units the complex becomes fully soluble and the polymerization rate increased. At high monomer conversion, a reactivity decrease is observed due to competitive complexation of *i*Bu₃Al by the polyether chain.⁴¹ Attempts to increase of the number of aluminum equivalents with respect to the benzyl alcohol did not led to significant improvement of the linearity of the kinetics. In order to scale the monomer reactivity, the plots of monomer conversion versus time have been superimposed in Figure 5. The presence of *i*Bu₃Al strongly modify the monomer reactivity scale: $k_{p,PO} > k_{p,BO} > k_{p,EEGE} \approx k_{p,AGE} > k_{p,BnGE} \approx k_{p,tBuGE}$. Trialkylaluminum deactivates the alkoxide propagating center but in the meantime activates the monomer through its coordination with the oxygen atom of the oxirane ring, which is increasing the electrophilicity of the α -methylene carbon. These opposing effects result in an overall improved reactivity of all the monomers, demonstrating the key role of monomer



complexation on the polymerization kinetics. The new reactivity scale can therefore be explained by the strength of the monomer coordination by $i\text{Bu}_3\text{Al}$ (Figure 6). For PO and BO, $i\text{Bu}_3\text{Al}$ can only be complexed by the oxygen atom of the epoxides ring resulting in strong monomer activation, high reactivity and fast polymerization. The activation of glycidyl ether monomers, such as EEGE and AGE, is reduced by the presence of additional oxygen atoms in the lateral substituent, which are also interacting with the Lewis acid and thus, slightly decreasing the expected electrophilicity of the α -methylene carbon, then their propagation rates. Similar reactivity differences have already been reported for the copolymerization of ethylene oxide (EO) with glycidyl ether monomers (EEGE and glycidyl methyl ether (GME)) under conventional oxyanionic or monomer-activated mechanisms.⁴² ⁴³ Lastly, the lower reactivity of $t\text{BuGE}$ and BnGE can be explain by the steric hindrance induced by their bulky side chain which is added to the complexation of the Lewis acid by the oxygen atoms of their side-chains. This hypothesis is supported by the fact that activated-monomer AROP mechanism is already proceeding through bulky aluminum complexes,⁴⁴ and by the bulkiness of $t\text{BuP}_4$,¹¹ which contributes to re-enforced the cumbersome environment around the propagating center.

Conclusions

Kinetics of the AROP of epoxyde monomers initiated by alcohol / $t\text{BuP}_4$ have been investigated. The propagating species have been identified to be exclusively ions pairs and the polymerization of epoxide monomers occurred via a living controlled polymerization process. A reactivity scale has been established for a library of 6 of the most commonly used epoxides monomers: 2 alkyl-substituted epoxides and 4 glycidyl ethers monomers: $k_{p,\text{BnGE}} > k_{p,\text{AGE}} > k_{p,\text{EEGE}} \gg k_{p,t\text{BuGE}} \approx k_{p,\text{PO}} > k_{p,\text{BO}}$. The epoxide lateral substituents have a significant influence on the monomer reactivity. Lateral substituents allowing an additional complexation of the phosphazanium couterions led to loose ion pairs and systems displaying higher reactivities. The addition of a Lewis acid in the reaction mixture, typical of monomer-activated ring-opening polymerization, led to an expected drastic increase of the kinetics but also to a full modification of the monomer reactivity scale due to differences in the strength of the monomer activation: $k_{p,\text{PO}} > k_{p,\text{BO}} > k_{p,\text{EEGE}} \approx k_{p,\text{AGE}} > k_{p,\text{BnGE}} \approx k_{p,t\text{BuGE}}$.

Conflicts of interest

There are no conflicts to declare”.

Acknowledgements

H.D. acknowledges the Ph.D. scholarship offered by the China Scholarship Council (CSC).

Notes and references

1. A.-L. Brocas, C. Mantzaridis, D. Tunc and S. Carlotti, *Progress in Polymer Science*, 2013, **38**, 845-873.
2. J. Herzberger, K. Niederer, H. Pohlit, J. Seiwert, M. Worm, F. R. Wurm and H. Frey, *Chemical Reviews*, 2016, **116**, 2170-2243.
3. M. Viviani, N. L. Meereboer, N. L. P. A. Saraswati, K. Loos and G. Portale, *Polymer Chemistry*, 2020, DOI: 10.1039/c9py01735f.
4. S. Boileau, *Pergamon Press plc, Comprehensive Polymer Science: the Synthesis, Characterization, Reactions & Applications of Polymers.*, 1989, **3**, 467-487.
5. S. Penczek, M. Cypryk, A. Duda, P. Kubisa and S. Stomkowski, *Progress in Polymer Science*, 2007, **32**, 247-282.
6. N. Badi, L. Auvray and P. Guegan, *Advanced Materials*, 2009, **21**, 4054-4057.
7. W. N. Ottou, H. Sardon, D. Mecerreyes, J. Vignolle and D. Taton, *Progress in Polymer Science*, 2016, **56**, 64-115.
8. S. Hu, J. Zhao, G. Zhang and H. Schlaad, *Progress in Polymer Science*, 2017, **74**, 34-77.
9. M. K. Kiesewetter, E. J. Shin, J. L. Hedrick and R. M. Waymouth, *Macromolecules*, 2010, **43**, 2093-2107.
10. A. P. Dove, *ACS Macro Letters*, 2012, **1**, 1409-1412.
11. S. Boileau and N. Illy, *Progress in Polymer Science*, 2011, **36**, 1132-1151.
12. J. Zhao, D. Pahovnik, Y. Gnanou and N. Hadjichristidis, *Macromolecules*, 2014, **47**, 1693-1698.
13. N. Illy, S. Boileau, J. Penelle and V. Barbier, *Macromolecular Rapid Communications*, 2009, **30**, 1731-1735.
14. H. Schlaad, H. Kukula, J. Rudloff and I. Below, *Macromolecules*, 2001, **34**, 4302-4304.
15. J. Zhao, H. Alamri and N. Hadjichristidis, *Chemical Communications*, 2013, **49**, 7079-7081.
16. L. Dentzer, C. Bray, S. Noinville, N. Illy and P. Guégan, *Macromolecules*, 2015, **48**, 7755-7764.
17. Ö. Tezgel, S. Noinville, V. Bennevault, N. Illy and P. Guégan, *Polymer Chemistry*, 2019, **10**, 776-785.
18. Ö. Tezgel, V. Puchelle, H. Du, N. Illy and P. Guégan, *Journal of Polymer Science Part A: Polymer Chemistry*, 2019, **57**, 1008-1016.
19. L. Hassouna, N. Illy and P. Guegan, *Polymer Chemistry*, 2017, **8**, 4005-4013.

20. B. Eßwein, N. M. Steidl and M. Möller, *Macromolecular Rapid Communications*, 1996, **17**, 143-148.
21. H. Misaka, E. Tamura, K. Makiguchi, K. Kamoshida, R. Sakai, T. Satoh and T. Kakuchi, *Journal of Polymer Science Part A: Polymer Chemistry*, 2012, **50**, 1941-1952.
22. T. Isono, S. Asai, Y. Satoh, T. Takaoka, K. Tajima, T. Kakuchi and T. Satoh, *Macromolecules*, 2015, **48**, 3217-3229.
23. S. Rassou, N. Illy, O. Tezgel and P. Guégan, *Journal of Polymer Science Part A: Polymer Chemistry*, 2018, **56**, 1091-1099.
24. H. Zhang, S. Hu, J. Zhao and G. Zhang, *European Polymer Journal*, 2017, **95**, 693-701.
25. A.-L. Brocas, A. Deffieux, N. Le Malicot and S. Carlotti, *Polymer Chemistry*, 2012, **3**, 1189-1195.
26. V. Rejsek, P. Desbois, A. Deffieux and S. Carlotti, *Polymer*, 2010, **51**, 5674-5679.
27. A. O. Fitton, J. Hill, D. E. Jane and R. Millar, *Synthesis-Stuttgart*, 1987, 1140-1142.
28. B. J. Schmitt and G. V. Schulz, *European Polymer Journal*, 1975, **11**, 119-130.
29. M. Szwarc and J. J. Hermans, *Journal of Polymer Science Part B: Polymer Letters*, 1964, **2**, 815-818.
30. H. Hostalka, R. V. Figini and G. V. Schulz, *Makromolekulare Chemie*, 1964, **71**, 198-203.
31. A. Stolarzewicz and D. Neugebauer, *Macromol. Chem. Phys.*, 1999, **200**, 2467-2470.
32. M. Erberich, H. Keul and M. Möller, *Macromolecules*, 2007, **40**, 3070-3079.
33. B. A. Rozenberg, Berlin, Heidelberg, 1986.
34. C. J. Chang, R. F. Kiesel and T. E. Hogen-Esch, *Journal of the American Chemical Society*, 1973, **95**, 8446-8448.
35. V. A. Ponomarenko, A. M. Khomutov, S. I. Il'chenko and A. V. Ignatenko, *Polymer Science U.S.S.R.*, 1971, **13**, 1735-1740.
36. B. F. Lee, M. Wolffs, K. T. Delaney, J. K. Sprafke, F. A. Leibfarth, C. J. Hawker and N. A. Lynd, *Macromolecules*, 2012, **45**, 3722-3731.
37. K. Roos and S. Carlotti, *European Polymer Journal*, 2015, **70**, 240-246.
38. C. Billouard, S. Carlotti, P. Desbois and A. Deffieux, *Macromolecules*, 2004, **37**, 4038-4043.
39. A. Labbé, S. Carlotti, C. Billouard, P. Desbois and A. Deffieux, *Macromolecules*, 2007, **40**, 7842-7847.
40. S. Carlotti, C. Billouard, E. Gautriaud, P. Desbois and A. Deffieux, *Macromolecular Symposia*, 2005, **226**, 61-68.
41. M. Gervais, A.-L. Brocas, G. Cendejas, A. Deffieux and S. Carlotti, *Macromolecules*, 2010, **43**, 1778-1784.
42. J. Herzberger, D. Leibig, J. C. Liermann and H. Frey, *ACS Macro Letters*, 2016, **5**, 1206-1211.
43. S. S. Müller, C. Moers and H. Frey, *Macromolecules*, 2014, **47**, 5492-5500.
44. V. Rejsek, D. Sauvanier, C. Billouard, P. Desbois, A. Deffieux and S. Carlotti, *Macromolecules*, 2007, **40**, 6510-6514.